Neurobiology of Disease 124 (2019) 133–140

Contents lists available at ScienceDirect

Neurobiology of Disease

journal homepage: www.elsevier.com/locate/ynbdi

Reduction of matrix metalloproteinase 9 (MMP-9) protects motor neurons from TDP-43-triggered death in rNLS8 mice

Krista J. Spiller[a,*], Tahiyana Khan[a], Myrna A. Dominique[a], Clark R. Restrepo[a], Dejania Cotton-Samuel[a], Maya Levitan[a], Paymaan Jafar-Nejad[b], Bin Zhang[a], Armand Soriano[b], Frank Rigo[b], John Q. Trojanowski[a], Virginia M.-Y. Lee[a]

[a] Center for Neurodegenerative Disease Research, Department of Pathology and Laboratory Medicine, University of Pennsylvania, Philadelphia, PA 19104, USA
[b] Ionis Pharmaceuticals, Carlsbad, CA 92010, USA

ARTICLE INFO

Keywords:
TDP-43
Motor neuron
MMP-9
rNLS8 mice
Amyotrophic lateral sclerosis (ALS)
Antisense oligonucleotide
AAV

ABSTRACT

Therapeutic strategies are needed for the treatment of amyotrophic lateral sclerosis (ALS). One potential target is matrix metalloproteinase-9 (MMP-9), which is expressed only by fast motor neurons (MNs) that are selectively vulnerable to various ALS-relevant triggers. Previous studies have shown that reduction of MMP-9 function delayed motor dysfunction in a mouse model of familial ALS. However, given that the majority of ALS cases are sporadic, we propose preclinical testing in a mouse model which may be more clinically translatable: rNLS8 mice. In rNLS8 mice, neurodegeneration is triggered by the major pathological hallmark of ALS, TDP-43 mislocalization and aggregation. MMP-9 was targeted in 3 different ways in rNLS8 mice: by AAV9-mediated knockdown, using antisense oligonucleotide (ASO) technology, and by genetic modification. All 3 strategies preserved the motor unit during disease, as measured by MN counts, tibialis anterior (TA) muscle innervation, and physiological recordings from muscle. However, the strategies that reduced MMP-9 beyond the motor unit lead to premature deaths in a subset of rNLS8 mice. Therefore, selective targeting of MMP-9 in MNs could be beneficial in ALS, but side effects outside of the motor circuit may limit the most commonly used clinical targeting strategies.

1. Introduction

Despite exciting new advancements in the understanding of the pathogenesis of amyotrophic lateral sclerosis (ALS), the disease remains uniformly fatal. Several drug candidates were considered promising in preclinical studies, but most have failed to show significant benefit to patients in clinical trials. A possible explanation for the mismatch between preclinical and clinical outcomes is that nearly all preclinical screening has been done in a mouse model of ALS with a mutation found in only about 2% of all ALS cases (that is, mice bearing a mutation in SOD1) (Benatar, 2007). To discover and validate therapeutic targets for ALS with a greater chance of successful clinical translation, it will be useful to test the same targets in multiple different disease models.

A new mouse model of ALS that should be particularly valuable for drug screening studies, is one that is based on what is likely a final common pathway for ALS disease subtypes: cytoplasmic TDP-43 mislocalization and aggregation (Mackenzie et al., 2007). In rNLS8 mice, neuron-specific expression of *hTDP43ΔNLS* results in the accumulation of abundant insoluble, phosphorylated TDP-43 in the brain and spinal cord (SC) with loss of endogenous nuclear TDP-43, and progressive motor impairments leading to death over approximately 10 weeks (Walker et al., 2015; Spiller et al., 2016a). Therefore, given that the disease is triggered by the major pathological hallmark of ALS, rather than a specific familial mutation, findings in this model may be applicable to most (sporadic) ALS cases. Further, these mice are well-suited for preclinical testing because the transgene is induced by removing doxycycline (DOX) from the animals' diet for easy manipulation prior to an adult-onset disease (e.g. a prevention study).

Though pathological TDP-43 is present in over 95% of ALS post-mortem cases (Neumann et al., 2006), targeting TDP-43 itself is a difficult strategy because its proper function is needed for cell function

Abbreviations: rNLS8 mice, regulatable NLS double transgenic line (NEFH-hTDP-43ΔNLS); TA, tibialis anterior muscle; GC, gastrocnemius muscle; CMAP, compound muscle action potential; SC, spinal cord; MN, motor neuron; MMP-9, matrix metalloproteinase-9; ASO, antisense oligonucleotide; NMJs, neuromuscular junctions; DOX, doxycycline; Tg, transgenic; i.m., intramuscular

* Corresponding author.
E-mail address: spillerk@upenn.edu (K.J. Spiller).

https://doi.org/10.1016/j.nbd.2018.11.013
Received 17 September 2018; Received in revised form 10 November 2018; Accepted 16 November 2018
Available online 17 November 2018
0969-9961/

and TDP-43 levels are autoregulated (Budini and Buratti, 2011). Therefore, new targets are needed for drug development. One potential target is matrix metalloproteinase 9 (MMP-9). MMP-9 has been previously shown to be expressed specifically in the motor neurons (MNs) that are most vulnerable to ALS (Kaplan et al., 2014; Spiller et al., 2016b). Moreover, removing MMP-9 entirely by genetic knock-out or reducing it by ~50% in all cells has been shown to slow disease and prolong lifespan in $SOD1^{G93A}$ mice (Kaplan et al., 2014; Kiaei et al., 2007). Of note, however, neither $SOD1^{G93A}$ mice, nor patients with a mutation in *SOD1*, have the pathology that is associated with the vast majority of patients (TDP-43 mislocalized to the cytoplasm and associated with ubiquinated inclusions) (Robertson et al., 2007), prompting concern over their validity for modeling human disease. We now report studies to test MMP-9 reduction in rNLS8 mice, extending those prior findings to sporadic ALS. We use 3 different strategies to do this, which range from very specific to very broad. First, we targeted a specific motor pool (that is, all of the MNs that connect to an individual muscle), using an intramuscular (i.m.) injection with an AAV9 vector expressing shRNA against Mmp9 ("AAV9.shMMP9"). Next, we used a single intracerebroventricular (i.c.v.) injection with antisense oligonucleotides to suppress gene expression of *Mmp9* throughout the rNLS8 central nervous system. Finally, we crossed $Mmp9^{-/-}$ mice with rNLS8 mice to achieve full MMP-9 removal in the triple transgenic offspring.

2. Materials and methods

2.1. Tg and nTg mice

As described previously (Walker et al., 2015), rNLS8 mice were generated by crossing Tg lines overexpressing tetracycline transactivator (tTA) protein under the control of the human *NEFH* promoter with an existing Tg line that can be induced with DOX manipulation to express human TDP-43 with a defective nuclear localization signal (*hTDP-43ΔNLS*). A DOX diet (Dox Diet #3888, Bio-Serv) inhibits tTA from binding to the tetracycline promoter element, repressing hTDP-43 expression. When mice are taken off DOX and given standard chow (Rodent Diet 20 #5053, PicoLab), hTDP-43 expression is activated. For the genetic studies, rNLS8 mice were crossed with mice heterozygous for an *Mmp9* gene disruption (B6.FVB(Cg)-$Mmp9^{tm1Tvu}$/J), on a C57BL/6J background. The resultant offspring were rNLS8;$Mmp9^{+/+}$, rNLS8;$Mmp9^{+/-}$, and rNLS8;$Mmp9^{-/-}$, and these littermates were directly compared for the experiments described in Fig. 4. For all studies, male and female mice were used and experimenters were blinded to the genotype/treatment of each mouse during data collection and identities were decoded later for analysis, using identification numbering based on toe tattooing. All procedures were performed in accordance with the NIH Guide for the Care and Use of Experimental Animals. Studies were approved by the Institutional Animal Care and Use Committee of the University of Pennsylvania. Timelines for individual experiments that show when MMP-9 was targeted relative to *hTDP43ΔNLS* expression can be found in Supplementary Fig. 1.

2.1.1. Intramuscular (i.m.) injections

Virus experiment: AAV9-CMV-PI-eGFP-WPRE-bGH (3.3×10^{13} gc/mL, Penn Vector Core) or AAV9-CMV-GFP-H1– MMP9-shRNA (9.47×10^{13} vg/mL, Virovek, Lot#15–170) were thawed on ice. P4 pups were anesthetized by hypothermia and, using a 31 gauge 1/2 cc insulin syringe (BD Ultra-Fine* II Short Needle Insulin Syringe, VWR), 2 µL of virus was injected into the TA. Pups were returned to their mother and their health was monitored to adulthood.

Retrograde tracing: 4 µL of cholera toxin subunit B (CTB) conjugated to Alexa Fluor 594 was injected into the TA muscle of the mice. CTB travels retrogradely from muscle to the MNs that innervate the injected muscle (L3 level of lumbar SC for TA). 4.5 days after the i.m. injection, the mice were perfused with PBS, followed by 4% PFA, for analysis of the lumbar SC. In all injected mice, the TA motor pool was fluorescently labeled with Alexa Fluor 594.

2.2. Muscle physiology

To perform the CMAP recordings, mice were anesthetized and their hind legs were shaved. The sciatic nerve was stimulated through bipolar needle electrodes by injecting brief electrical currents (0.3 Hz, 0.5 ms pulse duration, starting at 0 and incrementally increasing by 5 mA). The response from the gastrocnemius (GC) muscle was recorded using needle electrodes placed in the center of the muscle and in the tendon. The M-wave was measured at each escalating amplitude, until the maximal response was elicited and did not increase further.

2.3. Antisense oligonucleotides

After deeply anaesthetizing 3–4 month old rNLS8 or nTg mice with a ketamine/xylazine/ acepromazine mixture, they were immobilized in a stereotaxic frame (Kopf) and stereotaxic i.c.v. injections were made using predetermined coordinates (Bregma 0.3 mm, lateral +1 mm, and depth −3 mm) to inject into the lateral right ventricle with a Hamilton syringe under aseptic conditions. Mice were injected with either ASO-ctnrl (50 mg/mL) or ASOxMMP9 (50 mg/mL) in a final volume of 10 µL and the experimenter waited 5 min before pulling out needles. All injected animals were observed during and after surgery, and an analgesic was administered post-surgery.

2.4. Treadscan gait analysis

Gait analyses were performed using the TreadScan software from the CleverSys NeurodegenScan Suite. The BcamCap image capture system records the footprints of the mice walking/running across a transparent treadmill using a high-speed camera at 100 frames per second. The track speed was started at 5.0 cm/s and slowly increased until the mouse can no longer keep pace or until the track reached 18.0 cm/s. By tracking the footprints of the animals, the system identified which foot was placed on the track and for how long by frame. The software's video analyses gave parameters such as bilateral stance time and stride frequency, and instantaneous running speed. These data were then exported from the software into Microsoft Excel for statistical analyses by group and across time.

2.5. Immuofluorescence and quantification

rNLS8 mice and nTg controls were perfused with ice-cold PBS followed by 4% PFA and then the brain, lumbar SC and hindlimb muscles were surgically removed. Peripheral tissues were washed in PBS overnight, and the CNS tissue was post-fixed in 10% formalin overnight. All were then washed in PBS and then processed in a sucrose gradient up to 30% for cryoprotective embedding. To analyze MN populations in the brainstem and lumbar SC, tissues were sectioned at 20 µm and immunostained using the following primary antibodies: guinea pig anti-VAChT (1:1000, CNDR), rabbit anti-VAChT (1:5000, CNDR), mouse anti-human TDP-43 monoclonal antibody (MAb) (0.06 µg/mL, CNDR, clone 5104), goat anti-MMP-9 antibody (1:2000, Sigma-Aldrich), rabbit anti-p409-410 (pTDP-43 phosphorylated at Ser409/Ser410, 1:5000, Cosmo Bio Co.), and mouse anti-c-fos (1:100, Santa Cruz Biotechnology).

After overnight incubation with primary antibodies, tissue sections were washed and then incubated with Alexa Fluor secondary antibodies (1:1000, Molecular Probes). Sections were either imaged using a Nikon Eclipse Ni inverted microscope or a Leica TCS SPE. For the confocal imaging of microglia, 10 *z*-steps spaced 1–3 µm apart were collected per image and a maximum projection was created for each. For the quantification of MN numbers, MNs were counted in transverse 20 µm cryosections, 100 µm apart, over the length of 1 mm, using Image J and NIS-Elements software.

The tibialis anterior (TA) muscle was sectioned at 30 μm longitudinally, and immunostained with VAChT to label nerve terminals and α-bungarotoxin conjugated to Alexa-488 (BTX, 1:1000) to label motor endplates. The percentage of NMJ innervation was determined by dividing the total number of areas of overlap between VAChT and BTX signals (total number innervated endplates) by the number of areas of BTX signal (total number of endplates) on consecutive longitudinal 30 μm cryosections of muscles. We observed 500–1000 NMJs per TA.

2.6. Statistics

All experiments described in this paper were performed once. Data were first checked for normality (Shapiro-Wilk test) and Equal Variance (Brown-Forsythe test). Statistical significance was determined using paired *t*-tests for AAV experiments, unpaired two tail t-tests when comparing two separate groups in all other experiments, log rank survival analysis for the survival study shown in Fig. 4A, and one-way ANOVA when comparing multiple groups, using SigmaPlot. For significant results by one-way ANOVA, all pairwise multiple comparisons were made using the Holm-Sidak method. A p-value of < 0.05 was considered significant.

3. Results

3.1. Pool-specific MMP-9 knock-down protects the injected muscle from axonal dieback after 6 weeks of transgene expression

In order to experimentally knock-down MMP-9 in rNLS8 mice, P4 pups that resulted from the cross of NEFH8 X NLS4 males and females were injected with AAV9.CMV-GFP-H1-MMP9shRNA (from Virovek, Lot # 15–170, titer: 9.47×10^{13} gc/mL) or AAV9.CMV.PI.eGFP.WPRE.bGH (3.3×10^{13} gc/mL, Penn Vector Core) into their left TA muscle (Fig. 1A). When non-transgenic (nTg) or monogenic littermates reached adulthood, n = 8 were sacrificed to confirm viral transduction of MNs in the SC as well as MMP-9 expression levels in those transduced cells. When AAV9.shMMP9 was delivered into the TA motor pool (which typically has > 90% MMP-9$^+$ MNs), the number of MMP-9 negative TA-MNs was increased by about 36% after the AAV9.shMMP9 injection compared to AAV9.GFP injected controls (Fig. 1B-C). Of those that were still MMP-9 positive after being transduced with the silencing virus, the MNs were equally split between those that were considered MMP-9^{hi} versus MMP-9^{lo}.

After confirming the efficacy of the virus, we next waited for a group of AAV9.shMMP9-injected rNLS8 mice (n = 5) to reach adulthood (~P100), and removed DOX from their diet to initiate *hTDP43ΔNLS* expression. After 6 weeks off DOX, we recorded the maximum evoked CMAPs from the AAV9.shMMP9-injected TAs and compared these to the contralateral, control TAs. We found that the side with knocked down MMP-9 had significantly larger peak-to-peak M-wave amplitudes (paired *t*-test, $t_4 = 4.08$, p = .02, Fig. 1D-E). Kinematic analyses of treadmill walking using TreadScan software also revealed a significant difference in stance time between left and right hind limbs in these mice (Fig. 1F). Consistent with this protection in motor function, we found a morphological preservation of NMJs in AAV9.shMMP9-injected TAs, relative to their contralateral TA (~15% more intact NMJs, $t_4 = 7.6$, p = .002, Fig. 1G-H). Thus, a pool-specific reduction in MMP-9 resulted in attenuated axonal dieback from the corresponding muscle at 6 weeks off DOX. We also checked the SC of injected rNLS8 mice for phosphorylated TDP-43 inclusions in MNs, but did not find any in TA-innervating MNs, regardless of whether MMP-9 was reduced or not (Fig. 1I). Because that pool is particularly vulnerable, it is possible that there has already been death of pTDP-43 positive MNS, but this seems unlikely, given that fewer than 1% of neurons ever expressed pTDP-43 at any time point that we investigated in rNLS8 mice, in agreement with other recent reports (Porta et al., 2018).

3.2. ASO-mediated MMP-9 knock-down attenuates neuromuscular defects in rNLS8 mice without premature deaths

To test the result of more widespread knockdown, control or test ASOs (ASO-cntrl or ASOxMMP9) were delivered to nTg and rNLS8 mice by a single i.c.v. injection when all animals were two months old (~P60). First, experiments in nTg mice allowed us to test target specificity, knock-down, and the general distribution of the ASOs. 2 weeks after ASO administration, ASOs targeting MMP-9 increased the number of MMP-9 negative MNs dramatically in brainstem motor nuclei, such as the facial nucleus (Fig. 2A) and by about 20% in lumbar SC (Fig. 2B). We also noted an obvious reduction in the number of MNs that were highly immunopositive for MMP-9 ("MMP-9^{hi}"), with the majority of MNs expressing MMP-9 in a range that we considered "MMP-9^{lo}". To again home in on the TA-motor pool as an example of a vulnerable set of MNs, we backfilled from the TA with CTB-594 and looked at the MMP-9 expression specifically in that pool (Fig. 2C). We found that ASOxMMP9 administration lowered the % of MNs that highly express MMP-9 from ~70% to ~11% (Fig. 2D). Finally, we wanted to find out how long these reductions in MMP-9 lasted, and so we sacrificed another group of nTg mice 9 weeks post-injection. Though it appeared that the effect was not as strong as it had been 2 weeks post-injection, there were still 40% more MMP-9^{lo} motor neurons in the ASOxMMP9-injected mice compared to ASO-cntrl, though the number of MMP-9 negative MNs were now the same in both groups (not shown).

Once we confirmed successful MMP-9 reduction, we next assessed phenotypic and histopathologic effects of this knockdown in adult rNLS8 mice (n = 19). ASOs (ASO-cntrl, n = 8 and ASOxMMP9, n = 11) were injected i.c.v. into adult animals that were continuously maintained on DOX to suppress the *hTDP43ΔNLS* transgene. 2 weeks later, DOX was removed from the chow of the rNLS8 mice to initiate neuronal *hTDP43ΔNLS* expression. From that point, we monitored the animals' body mass, clasping, and tremor behavior 2 times per week throughout the experiment. Unexpectedly, we began to observe a hyperactive, high-anxiety behavior that sometimes resembled possible seizure-like activity (tail stiffening, head nodding, etc.) in the worst affected mice, starting at about 2.5 weeks off DOX only in the ASOxMMP9 treated rNLS8 animals (Supplementary Movie 1). However, we were not able to perform electroencephalography to identify real seizure events in these mice. Further, this behavior was not observed in ASOxMMP9 treated nTg mice or rNLS8 animals prior to transgene initiation.

Moreover, rNLS8 mice treated with ASO-cntrl did not exhibit these behaviors, and were phenotypically indistinguishable from uninjected rNLS8 off DOX, suggesting that ASO treatment itself is not toxic. Fos mRNA (or "c-fos") is induced when the activity of neurons is increased, and also has been widely reported to be induced in the hippocampus of rats and mice after spontaneous or kindled seizures (Labiner et al., 1993; Morgan et al., 1987). We found increased c-fos expression in ASOxMMP9-treated rNLS8 mice that appeared to have the abnormal, hyperactive behavior between 2 and 3 weeks off DOX, but not in treated rNLS8 mice that made it to their experimental end-points without that behavior (Supplementary Fig. 2).

Overall, there was no obvious improvement in gross disease symptoms in terms of onset of hind limb clasping or disease-triggered weight loss. Further, 4 of the 11 rNLS8 mice that were treated with ASOxMMP9 died or had to be euthanized prior to their designated experimental endpoint (Table 1). However, in the remaining animals, we found that MMP-9 knockdown did preserve muscle function from 4 weeks off DOX, with a maximum evoked CMAP recorded from the GC muscle of the ASOxMMP9 treated rNLS8 mice that was significantly higher than ASO-cntrl-injected controls (Fig. 3A). When we examined whole muscle morphologically, we found that MMP-9 knockdown prior to *hTDP43ΔNLS* expression significantly attenuated TA denervation in rNLS8 mice (Fig. 3B), with > 20% more intact NMJs at 6 weeks off DOX in the ASOxMMP9-treated versus ASO-cntrl-treated rNLS8 mice (72.5 ± 7 vs. 52.1 ± 9%, p = .04). Finally, MMP-9 knockdown by

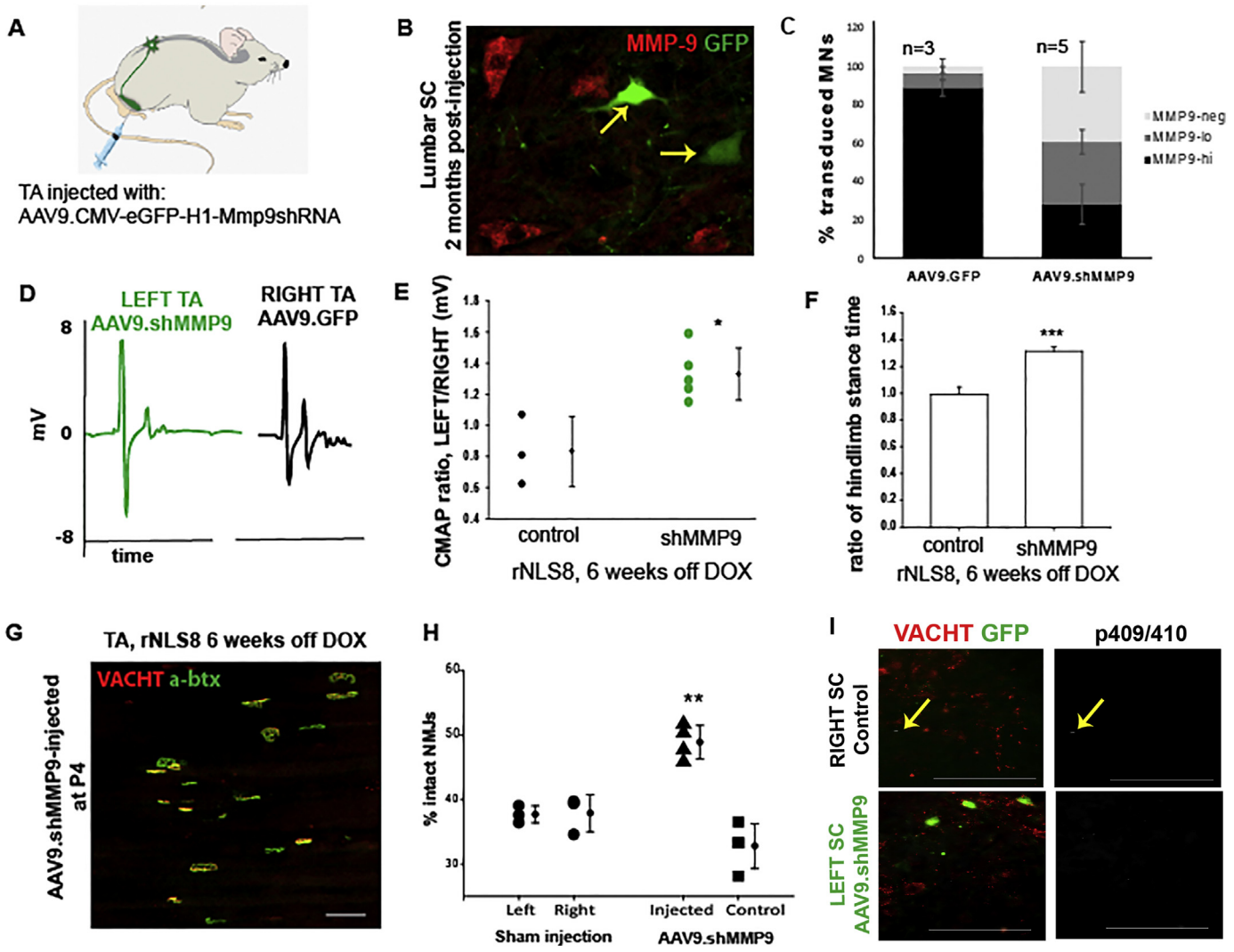

Fig. 1. Motor pool-specific MMP-9 knock-down protects the injected muscle from axonal dieback after 6 weeks of transgene expression. (A) rNLS8 mice at P4 were injected unilaterally into the TA with AAV9.shMMP9 (titer: 9.47×10^{13} vg/mL, custom made by Virovek, Inc.) to achieve pool-specific knockdown of MMP-9. (B) Representative cryosection of lumbar SC, 2 months after AAV9.shMMP9 administration, shows that GFP transduced MNs (green, arrow) are not MMP-9 positive (red). (C) AAV9.shMMP9 i.m. administration leads to a 36% reduction in the total number of $MMP9^{+}$ MNs ($t_6 = -4.5$, $p = .004$), and a 60% reduction in the numbers of $MMP\text{-}9^{hi}$ ($t_6 = 9.6$, $p < .001$). Bars show mean ± S.D., n = 3–5. (D-E) The amplitude of the maximum evoked CMAP was 23.9 ± 9% larger from the left TA (green, AAV9.shMMP-9-injected) compared to the right (black, control) TA. Individual points show the ratio of left to right CMAPs for each animal. Bars are mean ± S.D., n = 3–5. (F) While control animals have symmetrical paw placement (ratio close to 1) as they run on a treadmill, gait analysis software shows an imbalance of motor function in left versus right hind limbs (ratio: 1.3) in rNLS8 mice injected unilaterally with AAV9.shMMP9 at 6 weeks off DOX ($t_6 = -10.2$, $p < .001$). Bars show mean ± S.D., n = 3–5. (G-H) The overlap of VAChT-positive motor terminals (red) with acetylcholine receptors stained using BTX (green) was used as an indicator of innervated motor endplates. The percent innervation of TAs following 6 weeks of transgene expression shows that the left TA is protected after injection with AAV9.shMMP9 (triangles) compared to its uninjected TA (squares). Note that the control rNLS8 mice had symmetric muscle denervation (circles). (I) Representative images of lumbar SC from an rNLS8 mouse that given a unilateral i.m. injection with AAV9.shMMP9 and 6 weeks off DOX immunostained for pTDP-43 (p409/410, white) shows a rare instance of a pTDP-43 inclusion in a neuron which is not a MN in the uninfected side of lumbar SC (top panels, indicated with a yellow arrow). Very few pTDP-43 inclusions were detected at the lumbar level of SC, regardless of the MMP-9 levels. Bars represent mean ± S.D., n = 5 for AAV9.shMMP9 animals. Scale bar = 100 μm. (For interpretation of the references to colour in this figure legend, the reader is referred to the web version of this article.)

ASOxMMP9 also prevents MN loss at 6 weeks off DOX in rNLS8 lumbar SC, with an average of 16.9 ± 0.5 MNs per ventral horn in ASOxMMP9 mice versus only 14.4 ± 0.5 in the ASO-cntrl-injected mice (Fig. 3C). Therefore, ASO-mediated MMP-9 knock-down did attenuate neuromuscular defects in all of the assays we investigated in rNLS8 mice that survived to their experimental end-point. However, we cannot exclude the possibility that the ASOxMMP9-treated rNLS8 group measures only appeared higher because the most vulnerable 1/3 of mice died prematurely and were therefore not included in analyses.

Next, in order to test whether the "seizure-like" phenotype is an interaction of the TDP-43 disease phenotype with either the Mmp9 knock down or an ASO off target effect, we imported *Mmp9*$^{-/-}$ mice into our colony and crossed them with rNLS8 mice.

3.3. Genetic MMP-9 reduction attenuates neuromuscular defects, but has unwanted side effects in rNLS8 animals

Mmp9$^{-/-}$ mice are normal with no apparent gait defects (Supplementary Fig. 3). When we crossed these with rNLS8 mice to generate triple Tg mice, we found that the resultant rNLS8;*Mmp9*$^{-/-}$ have more premature deaths than littermates with MMP-9 (Fig. 4A), potentially suggesting that the early deaths in some of the ASOxMMP9-

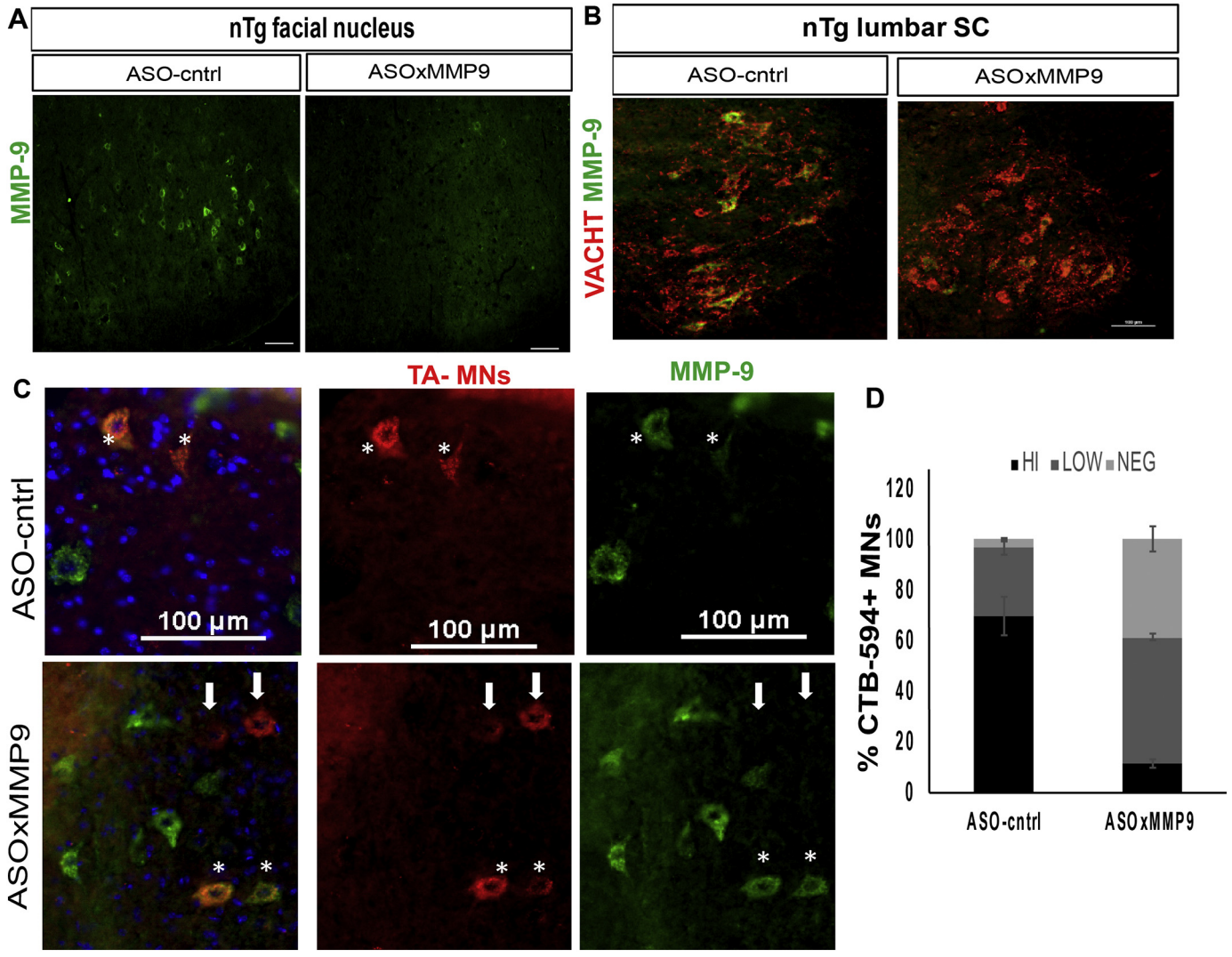

Fig. 2. A single i.c.v. injection of an ASO targeting *Mmp9* results in widespread MMP-9 reduction in nTg controls. (A) Representative pictures of nTg brains immunostained with MMP-9 (green) shows a marked decrease in the number of MMP-9-positive MNs in the facial nucleus at 2 weeks post injection. Similar staining was observed in 4 replicates. (B) There was also a decrease in the number of MMP-9-positive MNs (stained with VAChT, red) compared to the ASO-cntrl-treated controls at the lumbar level of SC in the same mice. (C-D). In the TA motor pool, identified by an i.m. injection with CTB-594 (red), there was about a 35% increase in the number of MMP-9 negative MNs (light grey) and the majority of remaining MNs only expressed a low level of MMP-9 (~55%, dark grey). MMP-9 negative MNs are indicated with white arrows, and asterisks show MMP-9 positive MNs. Bars show mean ± S.D. n = 3 animals with 2 TAs back-filled in each. Scale bars = 100 µm.

treated rNLS8 mice were not from some off-target effect, but rather because the ASOs were effective in targeting MMP-9 broadly. Like the ASO-xMMP-9 treated mice, rNLS8;*Mmp9*$^{-/-}$ had increased c-fos expression in the hippocampus when they were caught exhibiting seizure-like behavior between 2 and 3 weeks off DOX (Supplementary Fig. 2). Of the surviving mice, we found that rNLS8;*Mmp9*$^{+/+}$ mice can run faster than rNLS8;*Mmp9*$^{-/-}$ mice (Fig. 4B). In contrast to the apparent overall worsening of rNLS8 mice when MMP-9 is deleted, the evoked CMAP from the GCs were higher than in rNLS8 mice with MMP-9 intact (Fig. 4C) and MN death was attenuated (Fig. 4D-E). Therefore, though the connections between lumbar MNs and the hind limb muscles they innervate were preserved in the absence of MMP-9, the rNLS8 mice were generally worse off.

4. Discussion

Our results show that reducing MMP-9 in lumbar MNs delays axonal dieback and ameliorates ALS-relevant MN death in rNLS8 mice. These results agree with previous finding in the SOD1^{G93A} mouse (Kaplan et al., 2014), despite these lines having different triggers for MN death (that is, pathological TDP-43 versus mutant SOD1). This suggests that multiple different etiologies of ALS can elicit toxicity in the same predisposed vulnerable MN subtype (fast-fatigable MNs), and MMP-9 is in the pathway that mediates this toxicity. However, given that the protection is incomplete when MMP-9 is fully removed, these results suggest that MMP-9 is just one contributing factor to the selective vulnerability of fast MNs to TDP-43- (or mutant SOD1-) triggered degeneration. While evidence suggests that MMP-9 is indeed a contributing factor to MN vulnerability, MMP-9 and TDP-43 are unlikely to directly interact in non-pathological situations as MMP-9 acts primarily as a gelatinase in the extracellular space, and TDP-43 is a nuclear protein.

In contrast to previous findings in the SOD1^{G93A} mice, when the MMP-9 knockdown was more widespread than a single motor pool in rNLS8 mice, we found unexpected side effects that were sometimes fatal. Generally, in our colony, we see some baseline amount of premature death in the rNLS8 line (typically between 10 and 20% of animals), but what accounts for the fragility of this certain subset is not

Table 1
Experimental Subjects and inclusion in endpoint analysis.

	WT injected with ASOcntrl	WT injected with ASOxMMP9	rNLS8 injected with ASOcntrl	rNLS injected with ASOxMMP9
# Animals injected	6	7	8	11
# Animals that did not make it to their assigned end-point	0	0	0	4
% Included in complete study	100	100	100	64

Note: 1/3 of ASOxMMP9-treated rNLS8 animals, but not WT controls, died prior to their predetermined end-point.

known. However, the exacerbation of premature deaths that we see when MMP-9 levels are reduced could result from a few possible hypothetical mechanisms.

For example, given that we found a major upregulation in c-fos expression in the hippocampi of some rNLS8 with reduced MMP-9 levels (Supplementary Fig. 2), MMP-9's normal role for plasticity in the hippocampus could be a major contributing factor to potential seizure generation. Specifically, the formation of an epileptic focus has been shown to be impacted by impairments in the mossy fibers sprouting within the hippocampus (Koyama and Ikegaya, 2004), and MMP-9's role in this sprouting has been well-established (Wilczynski et al., 2008). Moreover, MMP-9 has direct effects on glutamatergic transmission by increasing the activity of the NMDA receptor through integrins (Bronisz and Kurkowska-Jastrzebska, 2016; Michaluk et al., 2009), another powerful way in which MMP-9 can functionally modify neuronal activity.

However, if the unwanted behavioral side effects resulted from just the loss of hippocampal MMP-9 function, ASOxMMP9 treatment would have adverse effects in nTg controls. This was not the case (Supplementary Video 1), and 100% of the ASOxMMP9-treated nTg mice were unaffected. Further, *Mmp9*$^{-/-}$ mice in our colony were grossly indistinguishable from *Mmp9*$^{+/+}$ littermates, suggesting that MMP-9 reduction alone does not trigger the hyperactive behavior in these mice either. Taken together, these results suggest the seizure-like effects could result from an interaction with the TDP-43-triggered dysfunction. Moreover, the generation of these behavioral events in the rNLS8 mice appears to happen within a fairly tight temporal window, between 2 and 3 weeks off DOX. This is the time period when endogenous mouse TDP-43 in lost from the nucleus of neurons (Walker et al., 2015), and presumably when those cells begin to experience loss-of-function effects. Around 2 weeks off DOX is also around the time that we notice subtle changes in cortical microglia morphology. Given that reactive microglia express MMP-9 in the brain (Konnecke and Bechmann, 2013), and that we have shown that microgliosis is protective in rNLS8 mice (Spiller et al., 2018), the loss of glial MMP-9 may very well be a factor in the generation of this behavioral phenotype in ASO-xMMP9-treated rNLS8 and rNLS8;*Mmp9*$^{-/-}$ animals.

Further, besides hippocampal plasticity and inflammation, MMP-9 has been shown to have many other homeostatic roles such as the regulation of growth factor activity (e.g. degradation of active NGF and conversion of pro-BDNF), Schwann cell migration, general tissue remodeling, and more (Bronisz and Kurkowska-Jastrzebska, 2016). The interference with these processes (or a combination of these processes) could also exacerbate the TDP-43-triggered vulnerability in rNLS8 mice.

Finally, we cannot exclude the possibility that the apparent benefits that we saw in terms of MN number and preserved functional NMJs are the result of a loss of the most vulnerable animals in the ASOxMMP9-treated and rNLS8;*Mmp9*$^{-/-}$ groups, not an actual protection conferred by MMP-9 reduction. However, the experiments with the AAV9.shMMP9 strongly argue against that possibility, since the comparisons were made within animals in those experiments (rather than between groups of animals with different treatments or genotypes, Fig. 1). Moreover, the previous results showing a therapeutic effect of MMP-9 reduction in MNs without any confounding side effects further support our conclusion (Kaplan et al., 2014; Kiaei et al., 2007). Therefore, our results suggest that targeting MMP-9 may still be a useful therapeutic strategy in ALS, but a drug delivery system to target spinal MMP-9 only would be needed.

5. Conclusion

Motor pool-specific MMP-9 knock-down protects the motor unit from dysfunction due to pathological TDP-43.

Supplementary data to this article can be found online at https://doi.org/10.1016/j.nbd.2018.11.013.

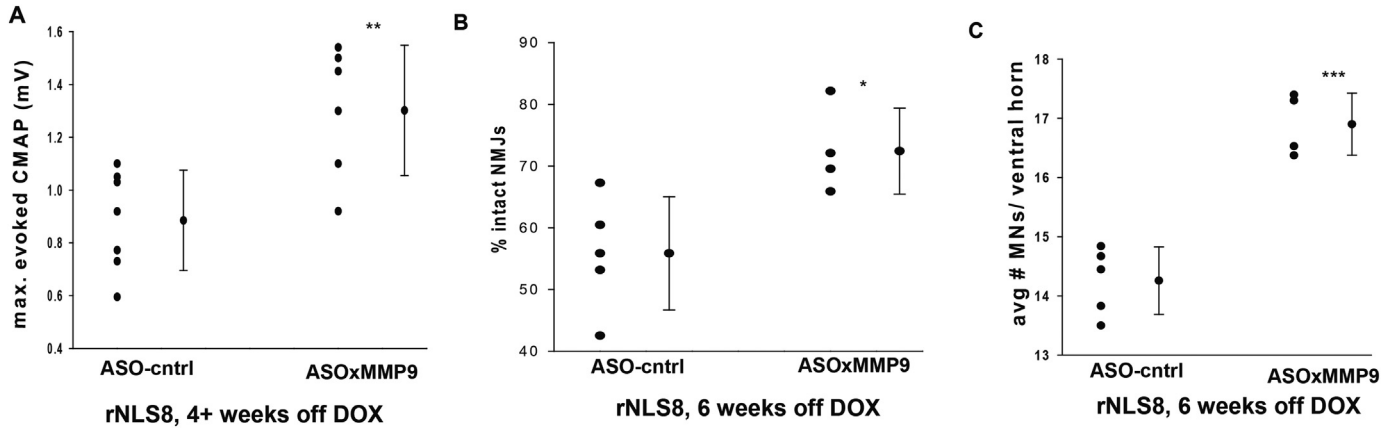

Fig. 3. ASO-mediated MMP-9 knock-down attenuates neuromuscular defects in rNLS8 mice in mice at 4–6 weeks off DOX. (A) Muscle recordings from the gastrocnemius muscle show more robust motor function in rNLS8 injected with the control ASO compared to those treated with ASOxMMP9 (**, $t_{11} = -3.3$, p = .007). (B) ASOxMMP9 treated rNLS8 mice have about 17% more intact NMJs in their TA muscles compared ASO-cntrl-treated rNLS8 mice (*, $t7 = -3.0$, p = .02). (C). There are significantly more MNs in ASOxMMP9 mice compared to control (***, $t_7 = -7.2$, $p < .001$). For all panels, individual data points are shown with bars indicating mean ± S.D. to the right.

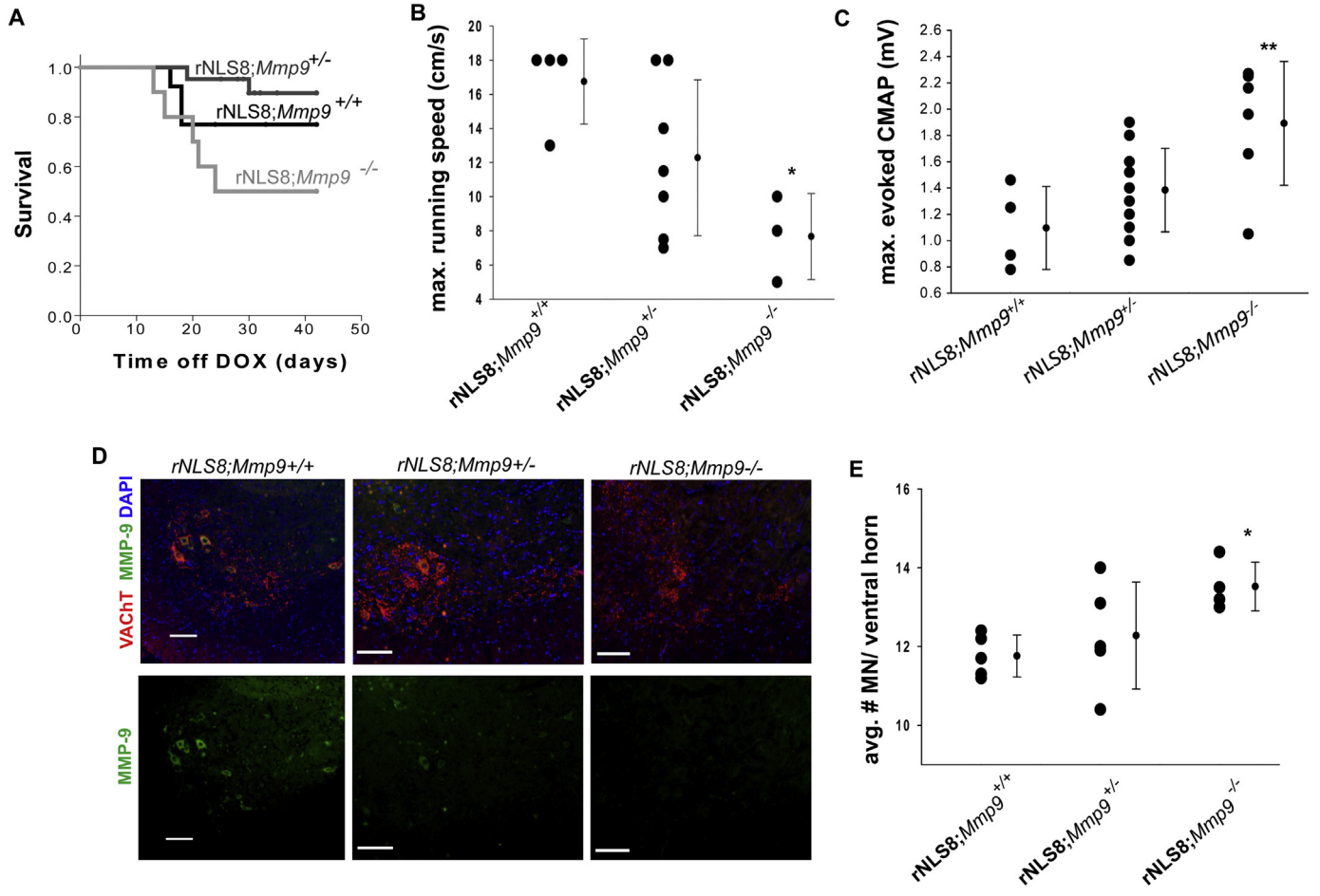

Fig. 4. MMP-9 reduction attenuates neuromuscular defects, but has unwanted side effects in rNLS8 animals. (A) rNLS8;*Mmp9*$^{-/-}$ mice have more premature deaths than littermates (Log-Rank test, p = .03), with half dying of suspected seizures between 2 and 3 weeks off DOX. (B) rNLS8;*Mmp9*$^{+/+}$ mice can run faster than rNLS8;*Mmp9*$^{-/-}$ mice at 5–6 weeks off DOX (*, One way ANOVA, $F_{2,11} = 5.1$, p = .03). (C) However, reducing MMP-9 preserves evoked compound muscle action potentials in rNLS8 mice (**, $F_{2,21} = 6.7$, p = .006). (D-E) Finally, deleting *Mmp9* attenuates MN death in rNLS8 mice(*, $F_{2,11} = 4.1$, p = .04). Representative cryosections (D) from lumbar SC of rNLS8;*Mmp9*$^{+/+}$, rNLS8;*Mmp9*$^{+/-}$, and rNLS8;*Mmp9*$^{-/-}$ littermates at 6 weeks off DOX immunostained with VAChT (red) to label MNs and MMP-9 (green) shows successful removal of MMP-9 in rNLS8;*Mmp9*$^{-/-}$. Scale bars = 100 µm. (E) Individual data points are shown with bars indicating mean ± S.D. to the right. (For interpretation of the references to colour in this figure legend, the reader is referred to the web version of this article.)

Conflict of interest statement

P.J.-N., A.S., and F.R. are employed by Ionis Pharmaceuticals, a for-profit company that develops ASO therapies. The other authors declare no competing financial interest.

Acknowledgements

We thank Target ALS for help in the design and acquisition of the AAV9.shMMP9 virus. We are extremely grateful to colleagues in CNDR and Biogen for helpful discussions and insights, particularly Kurt Brunden and Brigitte Pettmann. This work was supported by the ALS Association (K.J.S.) and a grant from the NIA/NIH (AG17586).

References

Benatar, M., 2007. Lost in translation: treatment trials in the SOD1 mouse and in human ALS. Neurobiol. Dis. 26 (1), 1–13.
Bronisz, E., Kurkowska-Jastrzebska, I., 2016. Matrix metalloproteinase 9 in epilepsy: the role of neuroinflammation in seizure development. Mediat. Inflamm. 2016, 7369020.
Budini, M., Buratti, E., 2011. TDP-43 autoregulation: implications for disease. J. Mol. Neurosci. 45 (3), 473–479.
Kaplan, A., Spiller, K.J., Towne, C., et al., 2014. Neuronal matrix metalloproteinase-9 is a determinant of selective neurodegeneration. Neuron 81 (2), 333–348.
Kiaei, M., Kipiani, K., Calingasan, N.Y., et al., 2007. Matrix metalloproteinase-9 regulates TNF-alpha and FasL expression in neuronal, glial cells and its absence extends life in a transgenic mouse model of amyotrophic lateral sclerosis. Exp. Neurol. 205 (1), 74–81.
Konnecke, H., Bechmann, I., 2013. The role of microglia and matrix metalloproteinases involvement in neuroinflammation and gliomas. Clin. Dev. Immunol. 2013, 914104.
Koyama, R., Ikegaya, Y., 2004. Mossy fiber sprouting as a potential therapeutic target for epilepsy. Curr. Neurovasc. Res. 1 (1), 3–10.
Labiner, D.M., Butler, L.S., Cao, Z., Hosford, D.A., Shin, C., McNamara, J.O., 1993. Induction of c-fos mRNA by kindled seizures: complex relationship with neuronal burst firing. J. Neurosci. 13 (2), 744–751.
Mackenzie, I.R., Bigio, E.H., Ince, P.G., et al., 2007. Pathological TDP-43 distinguishes sporadic amyotrophic lateral sclerosis from amyotrophic lateral sclerosis with SOD1 mutations. Ann. Neurol. 61 (5), 427–434.
Michaluk, P., Mikasova, L., Groc, L., Frischknecht, R., Choquet, D., Kaczmarek, L., 2009. Matrix metalloproteinase-9 controls NMDA receptor surface diffusion through integrin beta1 signaling. J. Neurosci. 29 (18), 6007–6012.
Morgan, J.I., Cohen, D.R., Hempstead, J.L., Curran, T., 1987. Mapping patterns of c-fos expression in the central nervous system after seizure. Science 237 (4811), 192–197.
Neumann, M., Sampathu, D.M., Kwong, L.K., et al., 2006. Ubiquitinated TDP-43 in frontotemporal lobar degeneration and amyotrophic lateral sclerosis. Science 314 (5796), 130–133.
Porta, S., Xu, Y., Restrepo, C.R., et al., 2018. Patient-derived frontotemporal lobar degeneration brain extracts induce formation and spreading of TDP-43 pathology in vivo. Nat. Commun. 9 (1), 4220.
Robertson, J., Sanelli, T., Xiao, S., et al., 2007. Lack of TDP-43 abnormalities in mutant SOD1 transgenic mice shows disparity with ALS. Neurosci. Lett. 420 (2), 128–132.
Spiller, K.J., Restrepo, C.R., Khan, T., et al., 2016a. Progression of motor neuron disease is accelerated and the ability to recover is compromised with advanced age in rNLS8 mice. Acta Neuropathol. Commun. 4 (1), 105.
Spiller, K.J., Cheung, C.J., Restrepo, C.R., et al., 2016b. Selective motor neuron resistance and recovery in a new inducible mouse model of TDP-43 proteinopathy. J. Neurosci. 36 (29), 7707–7717.
Spiller, K.J., Restrepo, C.R., Khan, T., et al., 2018. Microglia-mediated recovery from ALS-relevant motor neuron degeneration in a mouse model of TDP-43 proteinopathy. Nat. Neurosci. 21 (3), 329–340.
Walker, A.K., Spiller, K.J., Ge, G., et al., 2015. Functional recovery in new mouse models of ALS/FTLD after clearance of pathological cytoplasmic TDP-43. Acta Neuropathol. 130 (5), 643–660.
Wilczynski, G.M., Konopacki, F.A., Wilczek, E., et al., 2008. Important role of matrix metalloproteinase 9 in epileptogenesis. J. Cell Biol. 180 (5), 1021–1035.